# Two-Stage Dynamics of In Vivo Bacteriophage Genome Ejection

Yi-Ju Chen, 1,\* David Wu, 2,† William Gelbart, 3 Charles M. Knobler, 3 Rob Phillips, 2,4,‡ and Willem K. Kegel Department of Physics, California Institute of Technology, Pasadena, California 91125, USA
Division of Engineering and Applied Sciences, California Institute of Technology,
Pasadena, California 91125, USA
Department of Chemistry and Biochemistry, University of California,
Los Angeles, Los Angeles, California 90095, USA
Division of Biology and Biological Engineering, California Institute of Technology,
Pasadena, California 91125, USA
Van 't Hoff Laboratory for Physical and Colloid Chemistry, Debye Institute, Utrecht University,
Padualaan 8, 3584 CH Utrecht, The Netherlands

(Received 1 July 2017; revised manuscript received 27 January 2018; published 1 May 2018; corrected 18 May 2018)

Biopolymer translocation is a key step in viral infection processes. The transfer of information-encoding genomes allows viruses to reprogram the cell fate of their hosts. Constituting 96% of all known bacterial viruses [A. Fokine and M. G. Rossmann, *Molecular architecture of tailed double-stranded DNA phages*, Bacteriophage **4**, e28281 (2014)], the tailed bacteriophages deliver their DNA into host cells via an "ejection" process, leaving their protein shells outside of the bacteria; a similar scenario occurs for mammalian viruses like herpes, where the DNA genome is ejected into the nucleus of host cells, while the viral capsid remains bound outside to a nuclear-pore complex. In light of previous experimental measurements of *in vivo* bacteriophage  $\lambda$  ejection, we analyze here the physical processes that give rise to the observed dynamics. We propose that, after an initial phase driven by self-repulsion of DNA in the capsid, the ejection is driven by anomalous diffusion of phage DNA in the crowded bacterial cytoplasm. We expect that this two-step mechanism is general for phages that operate by pressure-driven ejection, and we discuss predictions of our theory to be tested in future experiments.

DOI: 10.1103/PhysRevX.8.021029 Subject Areas: Biological Physics,

Interdisciplinary Physics, Soft Matter

#### I. INTRODUCTION

Tailed double-stranded DNA bacteriophages [1] are often used as model systems to study the physics of tightly confined DNA polymers [2–7] and the material properties

On leave at Division of Engineering and Applied Sciences, California Institute of Technology, Pasadena, California 91125, USA and Division of Biology and Biological Engineering, California Institute of Technology, Pasadena, California 91125, USA.

Published by the American Physical Society under the terms of the Creative Commons Attribution 4.0 International license. Further distribution of this work must maintain attribution to the author(s) and the published article's title, journal citation, and DOI. of the viral capsid [8,9]. These properties provide the basis for a quantitative understanding of the trajectory of infection and development. While many works focus on viral DNA packaging into the procapsid [7,10–14], we turn here to its reverse process, the bacteriophage genome ejection, and aim to explain the features of ejection dynamics observed in recent *in vivo* experiments [15]. While we focus on phage lambda, it is expected that the results of our analysis are general for the class of phages where DNA ejection is driven by the internal pressure of the encapsulated DNA. Moreover, a better understanding of the dsDNA bacteriophage infection process may also shed light on the biophysics of viruses with similar architecture, such as dsDNA/dsRNA eukaryotic viruses [16] and dsDNA archaeal viruses, which comprise most known archaeal viruses [17].

In the last stages of viral infection, viral genomes and structural proteins are produced by different cellular machineries and then assemble into new viral particles. As opposed to self-assembly for many viruses, tailed bacteriophages, which have double-stranded DNA genomes, use energy-consuming molecular motors to package the genomes into the capsids and fill a large fraction (about 50%) of the

<sup>\*</sup>Present address: The Salk Institute, University of California, San Diego, La Jolla, California 92037, USA.

<sup>&</sup>lt;sup>†</sup>Present address: Department of Medicine, Section of Pulmonary and Critical Care Medicine, University of Chicago, Chicago, Illinois 60637, USA.

<sup>\*</sup>To whom correspondence should be addressed. phillips@pboc.caltech.edu

<sup>\*</sup>To whom correspondence should be addressed. w.k.kegel@uu.nl

volume [5,10–13]. Under physiological ionic conditions, the densely packed, negatively charged DNA exerts a pressure in the capsid (mainly from the repulsive "hydration force" between the confined DNA strands [18]) of up to tens of atm [3,10]. It is hypothesized that the pressurized DNA could later facilitate the genome ejection process when infecting a new host once the tail opens. The tens of atm pressure inside the capsid provides a driving force corresponding to tens of pN for DNA whose cross-sectional area is a few nm². However, our understanding of the mechanisms of bacteriophage genome ejection remains incomplete [3,19–24], especially with regard to delivery of the last portion of the genome.

Besides the internal energy originating from the hydration force, the DNA also stores elastic energy [2–5] because it is packed into the capsid whose internal radius ( $R \approx 30$  nm) is smaller than the DNA persistence length ( $\xi_p \approx 50$  nm). However, simple estimates show [3,5] that the direct contribution of the elastic energy to the ejection driving force is small compared to that from the repulsions between neighboring strand portions. Accordingly, in the present discussion, we will ignore the direct contribution of the elastic energy to the ejection kinetics.

In the case of bacteriophage  $\lambda$  genome ejection in vitro, a theoretical model built upon the hydration force given in Ref. [18] identified the ionic conditions and the amount of DNA remaining in the capsid as state variables for the ejection driving force [4,5]. It correctly predicted the geometry of the packaged DNA under different ionic conditions [6], as well as the osmotic pressure of the surrounding solution (generated by adding osmolytes to the solution) required to balance the self-repulsion of a given amount of DNA in the capsid and halt the ejection [25,26]. A measurement of the ejection dynamics in vitro—i.e., for purified viral capsids—also showed that the ejection speed scales with the amount of DNA in the capsid, regardless of the total genome length [27], agreeing with the idea that the ejection driving force (and frictional coefficient) should have the remaining amount of DNA in the virus as its state variable.

Here, as a model system to study the phage ejection process in vivo, we restrict the discussion to bacteriophage  $\lambda$ , being the only case where single-virus ejection into the host cells has been measured [15], and whose ejection driving force has been established [3–5,25–27]. One aim is to explain some features observed in our previous measurements of phage  $\lambda$  in vivo ejection speed [15] [Fig. 1(a) and inset]. We note, in particular, that the speed was found to be about two orders of magnitude slower than the in vitro ejection speed measured in Refs. [27,28]. Typical timescales for in vivo and in vitro ejection are a few minutes and a few seconds, respectively. Also, a gram-negative bacterium, such as the E. coli host for the  $\lambda$  phage, has a turgor pressure of 0.1–5 atm higher than the environment [29,30]. An osmotic pressure of the same magnitude was able to stop the ejection in the *in vitro* setting [25,26,31], but obviously, in vivo, the complete genome of the phage is

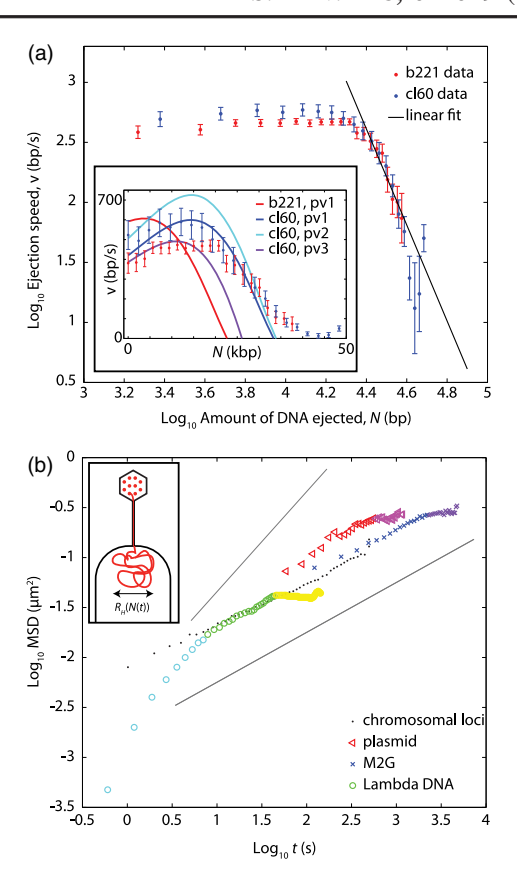


FIG. 1. Data on in vivo phage ejection and macromolecular diffusion. (a) Speed of phage in vivo ejection as a function of the amount of DNA ejected. The data from Ref. [15] are plotted on a log-log scale, suggesting two stages of behavior. A linear fit to the later stage gives  $\log v = (-3.99 \pm 1.67) \log N + (20.2 \pm 7.7)$ . The two  $\lambda$  phage mutants, cI60 and b221, were used for their different genome lengths. In the inset, the data plotted on a linear scale are compared with the results (solid curves) calculated for the early-stage ejection using different parameter sets in Eqs. (1)–(3), as explained in the text. The red and blue curves are phage b221 and cI60, respectively, with the same parameter values (pv) choice. Cyan and purple curves show how the phage cI60 curve changes when the parameters change. For pv1,  $p_0 = 6.58 \times 10^4$  kPa,  $P_b =$ 4.28 kPa; for pv2,  $p_0 = 1.2 \times 6.58 \times 10^4$  kPa,  $P_b = 4.28$  kPa; and for pv3,  $p_0 = 6.58 \times 10^4 \text{ kPa}$ ,  $P_b = 5 \times 4.28 \text{ kPa}$ . (b) Loci tracking of diffusing macromolecules in the live cells reported in the literature. The mean-squared displacement (MSD) as a function of time is plotted on a log-log scale. Black dot symbols represent bacterial chromosomal loci [32],  $\alpha = 0.4$ ,  $D_{\rm app} = 10^{-2} \ \mu {\rm m}^2/{\rm s}^{\alpha}$ . Red and pink left pointed triangle symbols represent plasmid (6 kbp, circular) [33]; red represents the subdiffusive regime,  $\alpha = 0.54$ ,  $D_{\rm app} = 8 \times 10^{-3} \ \mu {\rm m}^2/{\rm s}^{\alpha}$ . Blue and purple times symbols represent M2G (crescentin-GFP protein complex) [33]; blue represents the subdiffusive regime,  $\alpha = 0.44$ ,  $D_{\rm app} = 9 \times 10^{-3} \ \mu {\rm m}^2/{\rm s}^{\alpha}$ . Yellow, green, and cyan circle symbols represent phage  $\lambda$  DNA (50 kbp, circularized in the cell) searching for its specific integration site on the bacterial genome [34]; green represents the subdiffusive regime, slope  $\alpha = 0.5$ ,  $D_{app} = 6 \times 10^{-3} \ \mu \text{m}^2/\text{s}^{\alpha}$ . Yellow represents constrained diffusion of the phage DNA that remains anchored to the entry site after ejection. For reference, the two gray lines have slopes of 0.5 and 1, respectively. The logarithms are with base 10. Inset: The ejecting phage genome.

somehow being ejected [15]. Our model will provide an explanation for how phage  $\lambda$  ejection may continue after the net driving force disappears, without mechanisms that involve the enzymatic pulling found in phages T7 and  $\phi$ 29 [20–22]. Such an enzyme-catalyzed reaction has not been shown to drive phage  $\lambda$  ejection under physiological conditions, as far as we are aware. In addition, the rate of T7 DNA translocation catalyzed by *E. coli* RNA polymerase is constant and less than 80 bp/s at physiological temperature [20,21], while the  $\lambda$  genome ejection speed is changing and, for the most part, faster than 80 bp/s [see Fig. 1(a) inset].

Besides enzymatic pulling, passive DNA-binding agents in the cell may result in an adsorption force or a ratchet action on the phage genome and could potentially facilitate genome internalization [19]. However, both theoretical [19] and experimental (in vitro) [35] analyses show that the effect of DNA-binding agents is weak compared to that of DNA self-repulsion. Even in the later stage of ejection, where the DNA self-repulsion exhausts, the changing speed of in vivo ejection [shown in Fig. 1(a)] is not indicative of a mechanism based on DNA binding agents—which is expected to have a constant-speed behavior [19]. Another passive mechanism favoring ejection proposed in Ref. [36] is due to phage DNA condensation in a crowded environment and solvent exclusion generating an effective pulling force. However, if that were the dominating mechanism, the ejection force would grow with the amount of ejected DNA, inconsistent with the observed in vivo ejection speed, which decreases as ejection proceeds [Fig. 1(a)].

Figure 1(a) shows the measured in vivo ejection speed on a log-log scale, going from a higher-value plateau to a linearly decreasing velocity profile after roughly 25 kbp (10<sup>4.4</sup> bp) DNA have ejected. We identify these regimes with a pressure-driven regime, where the majority of DNA is still in the capsid, and a diffusive regime, where most of the DNA has been released into the cell. Note that the main difference between in vivo and in vitro scenarios is that the phage DNA ejected into a bacterium is in a collapsed state in the cytoplasm because of the macromolecular crowding and wrapping by nucleoid-associated proteins [37,38], while DNA ejected into an aqueous solution is well described by the wormlike chain model [39]. In the early regime, we invoke the DNA selfrepulsion as the main origin of the ejection driving force, but now working against the turgor pressure of bacteria. Also, the hydration force itself may be scaled down, depending on the ionic strength of the in vivo ejection buffer, resulting in the slower ejection speed. We propose that, after the driving term has been exhausted, the later stage of DNA ejection is a manifestation of selfdiffusion—more specifically, taking a form similar to what Fig. 1(b) shows, that is, subdiffusion of macromolecules in the crowded cellular environment.

## II. PRESSURE-DRIVEN EJECTION

To describe the early-stage behavior, the ejection of DNA is driven by its self-repulsion counteracted by the bacterial turgor pressure. The ejection speed is the result of a balance between the net driving force and the Stokes drag, being a frictional coefficient times the speed  $(\mu \cdot (dL/dt) = F_{\rm eff})$ . (A similar treatment was used in discussing the *in vitro* ejection dynamics of phage  $\lambda$  [27]). Therefore, the ejection speed of DNA can be written as

$$\frac{dL}{dt} = \frac{F(L) - \delta A \cdot P_b}{\mu_{\text{tot}}(L)},\tag{1}$$

where L(t) is the amount of DNA remaining in the capsid at time t, dL/dt is the ejection speed, and  $\mu_{\rm tot}(L)$  is the frictional coefficient. F(L) is the pressure-driven component of the force, for a length L of the genome confined in the capsid. The resisting force as the DNA enters the cell is approximated as the bacterial turgor pressure  $P_b$  times the cross-sectional area of the DNA molecule,  $\delta A$ .

For each DNA length L, the packaged genome is associated (see below) with a unique interaxial spacing  $d_s$  and, therefore, with an ejection force  $F(d_s(L))$ . The dependence of F on  $d_s$  for different ionic strength conditions has been measured in osmotic stress experiments [18] and fit to a simple analytical form in Refs. [3–5]. In the absence of polyvalent cations, and for physiological salt conditions, this hydration force pushing DNA out of the virus takes the form  $F(L) = \sqrt{3}p_0(c^2 + cd_s)e^{-(d_s/c)}$  [4,5].  $p_0$  and c are, respectively, the amplitude and decay length of the hydration force [18] between adjacent DNA strands separated by a distance  $d_s$ ,  $(1/\sqrt{3})p_0d_se^{-(d_s/c)}$  per unit length. The spatial organization of water molecules and ions near interfaces was suggested to be the origin of the hydration force [40]; however, the exact mechanism is still under debate [41–43]. We will treat  $p_0$  and c as empirical parameters that change with buffer conditions. For any given L, the authors of Refs. [3-5] assert that the packaged DNA is characterized by an interaxial distance  $d_s$  that minimizes the total energy of the DNA, and they derive  $d_s$ as a function of L accordingly. Interestingly, the authors of Ref. [5] also showed that, in many circumstances, we can approximate the total volume of packaged DNA by the volume of the phage capsid, so that the DNA occupies all available space. That is,  $d_s$  can be approximated by  $\sqrt{(2V_{\rm cap}/\sqrt{3})L^{-\frac{1}{2}}}$ , with  $V_{\rm cap}$  the volume of the capsid. Using this in the expression for F(L) gives

$$F(L) = \sqrt{3}p_0 c^2 \left[ 1 + \left( \frac{\sigma}{L} \right)^{\frac{1}{2}} \right] e^{-(\sigma/L)^{\frac{1}{2}}}, \tag{2}$$

where  $\sigma = (2V_{\rm cap}/\sqrt{3}c^2)$ .

To estimate the frictional coefficient  $\mu_{tot}$ , we note that it should have contributions from the part of DNA in the virus  $\mu_v$  and that in the bacterial cytoplasm  $\mu_b$ . Analogously, for in vitro phage ejection, the frictional coefficient should have contributions from DNA in the virus and DNA in the surrounding buffer. The frictional coefficient in the *in vitro* ejection setting has been measured and analyzed in detail in Refs. [27,39], and the contribution from DNA in the virus was found to be dominant. Therefore, we can use here the in vitro ejection frictional coefficient to approximate the  $\mu_v$  term for the in vivo ejection. The in vitro ejection frictional coefficient as a function of L measured in Ref. [27] is fit well by an exponential decay. The exponential fit gives  $\theta_1 e^{\theta_2 L}$ , where  $\theta_1 \approx 0.017 \; (\text{pN.s/kbp}) \; \; \text{and} \; \; \theta_2 \approx 0.094 \; (1/\text{kbp}), \; L \; \; \text{is} \; \; \text{in}$ kbp, and  $\mu_v$  is in (pN.s/kbp). We will adopt this as our functional form for  $\mu_v(L)$ .

For the contribution from the part of DNA in the bacterial cytoplasm, we estimate it using Stokes' law,  $\mu_b = 6\pi\eta R_H$ , where  $\eta$  is the dynamic viscosity of the cytoplasm and  $R_H$  is the hydrodynamic radius of the DNA "blob" in the crowded cytoplasm, taking the form  $R_H = \xi_p^{\frac{2}{3}} b^{\frac{1}{3}} (L_{\text{tot}} - L)^{\frac{1}{3}}$ , which we will explain in more detail later. We assume that condensation of ejected DNA onto the blob is fast compared to the ejection speed. Here  $\xi_p \approx 50$  nm is the persistence length of the DNA [44],  $b \approx 0.34$  (nm/bp) is the length of a base pair, and  $(L_{\text{tot}} - L)$  is the amount of DNA ejected into the cytoplasm. Note that  $(L_{\text{tot}} - L)$  is not the linear dimension of the ejected DNA. At the crossover where  $(L_{\text{tot}} - L) \approx 25$  kbp (8  $\mu$ m), the linear dimension of the ejected DNA is roughly the  $R_H$  given above, which is submicron. Combining these results, we have

$$\mu_{\text{tot}} = \mu_v + \mu_b = \theta_1 e^{\theta_2 L} + 6\pi \eta \xi_p^{\frac{2}{3}} b^{\frac{1}{3}} (L_{\text{tot}} - L)^{\frac{1}{3}}.$$
 (3)

We combine Eqs. (1), (2), and (3) to estimate the earlystage ejection speed, shown in the Fig. 1(a) inset. We estimate the cross-sectional area of the DNA molecule  $\delta A$ by taking its radius to be 1 nm, and we estimate the phage capsid volume  $V_{\text{cap}}$  by approximating the capsid as a sphere of radius 30 nm. The  $\lambda$  phage used in Ref. [15] is cI60 which is essentially the wild type, with  $L_{\text{tot}} = 48.5 \text{ kbp}$  and a shorter-genome mutant b221 that has  $L_{\text{tot}} =$ 37.8 kbp. The viscosity of the cytoplasm  $\eta = f\eta_0$  is higher than the viscosity of water,  $\eta_0 = 10^{-3} \text{ Pa} \cdot \text{s}$ . In E. coli cytoplasm,  $\xi_p \approx 50$  nm and  $f \approx 10$  based on the selfdiffusion of small protein molecules [44]. However, for larger macromolecules, the effective viscosity may be larger [33]. Using parameter values that are in reasonable agreement with previous studies [27,29,30] (c = 0.5 nm,  $p_0 = 6.58 \times 10^4$  kPa, and  $P_h = 4.28$  kPa) our model captures the measured early-stage behavior of phage cI60, as can be seen by the blue curve in the Fig. 1(a) inset.

Of course, we need to check the sensitivity of our results to the parameters in the model. To that end, in the Fig. 1(a) inset, we perform such a sensitivity analysis. If we vary the value of  $p_0$  and  $P_b$  for phage cI60, the cyan  $(p_0=1.2\times6.58\times10^4~\mathrm{kPa},P_b=4.28~\mathrm{kPa})$  and purple  $(p_0 = 6.58 \times 10^4 \text{ kPa}, P_b = 5 \times 4.28 \text{ kPa})$  curves in the Fig. 1(a) inset demonstrate how  $p_0$  affects the magnitude of the speed, and how  $P_b$  determines where the pressuredriven regime ends (when the speed goes to zero). In comparison, the  $P_h$  values we used, in the range of 4.28–21.4 kPa, are in reasonable agreement with the lower end of measured E. coli turgor pressure, 10-500kPa [29,30]. The purple curve in the Fig. 1(a) inset has  $P_b =$ 21.4 kPa and its pressure-driven regime ends at around 25 kbp (10<sup>4.4</sup> bp), which is roughly where the crossover from a plateaulike to a power-law behavior occurs [seen more easily on the log-log scale in Fig. 1(a)]. The 10-mM MgSO<sub>4</sub> and 10-mM NaCl buffers used in previous in vitro ejection experiments are found to have c = 0.3 nm,  $p_0 =$  $1.2 \times 10^7$  kPa and c = 0.52 nm,  $p_0 = 6.6 \times 10^5$  kPa, respectively [27]. Here, in the in vivo ejection setting, the cells and phages are in the "M9 buffer" [45] and the influences of the buffer composition on c and  $p_0$  are unknown. While c is of the same order of magnitude for other buffers, as with the value c = 0.5 nm we used here,  $p_0$  could differ by several fold. The M9 buffer has a higher ionic strength than the in vitro ejection buffers and may therefore have a smaller  $p_0$ , agreeing with the smaller value (in the range of  $p_0 - 1.2p_0 = 6.58 \times 10^4 - 7.90 \times 10^4 \text{ kPa}$ ) that we used here.

Using  $L_{\text{tot}} = 37.8$  kbp for phage b221 (all other parameters remained the same), our model generated the red curve in the Fig. 1(a) inset. In qualitative agreement with the b221 data, the predicted ejection speed is plateaulike in the early stage of ejection and then gradually vanishes. However, the predicted speed vanishes at significantly shorter times than observed in the experiments. In our model, since the driving force for ejection depends on the amount of DNA remaining in the capsid, the b221 curve is always in advance of the cI60 curve by roughly 11 kbp, but this feature is not seen in the data. Our model of a forcedriven ejection is not in agreement with the experimental data at the later stage. We note that as the ejection approaches the crossover between the plateaulike and the power-law regimes, there is roughly as much DNA left in the capsid as there is already ejected in the bacterial cell, but although we used a DNA "blob" to consider the friction in Eq. (3), we may not have fully accounted for the restricted mobility in the cell.

We also note that the quality of the fit for phage cI60 is better than that for phage b221. In calculating  $F(d_s(L))$ , we used the  $d_s(L)$  in the "no void" configuration, which worked well when the phage was in buffers that typically contain 10-mM Na<sup>+</sup> or Mg<sup>2+</sup> [5]. Since the M9 buffer used for the *in vivo* ejection measurement in Fig. 1(a) has more

than 100 mM of cations [15], this approximation for  $d_s(L)$ and, therefore,  $F(d_s(L))$  is not expected to be precise. Cations generally reduce the self-repulsion of the phage DNA, and the effect is expected to be more obvious for shorter L, which has a lower self-repulsion energy. It has been shown that adding 100-mM Na<sup>+</sup> to the buffer makes the b221 phage DNA more concentrated towards the capsid wall and, therefore, having smaller  $d_s(L)$  compared to the no-void configuration [6]: We speculate that at high salt condition, the DNA configuration in the capsid does not simply depend on L, but also on the initial condition, so the two phages have different driving forces and speed at the same L. That results in a less accurate fit for the b221 ejection speed compared to the situation for cl60. In spite of the lack of quantitative agreement for the shorter-genome phage, we have provided an explanation for the much slower in vivo ejection speed [15] compared to the in vitro ejection speed [27,28]. We also showed that the ejection driving force and the resultant ejection speed exhaust as ejection progresses, which justified our attributing the DNA motion in the later stage of ejection mainly to its subdiffusion in the cell.

#### III. DIFFUSIVE REGIME

We now examine the later stage of ejection and how it is related to anomalous diffusion of macromolecules. Recent tracking experiments [32-34,46-48] have shown that the macromolecules in the crowded cellular environment often exhibit subdiffusive transport, characterized by  $MSD = D_{app}t^{\alpha}$ , where  $\alpha < 1$ . In Fig. 1(b), we compare the motion for several macromolecules in the bacterial cytoplasm measured in Refs. [32–34], including chromosomal loci, plasmid, protein complexes, and bacteriophage  $\lambda$  DNA "searching" for its genome integration site. We report the exponent  $\alpha$  and apparent diffusion coefficients  $D_{\rm app}$  in the legend of Fig. 1(b). These species have  $\alpha$  in the range of 0.4–0.6. For bacteriophage  $\lambda$  ejection, we will assume that the part of the ejected DNA in the cytoplasm exhibits similar subdiffusive behavior and takes an average value of the exponents,  $\alpha \approx 0.5$ .

This subdiffusive behavior is largely attributed to the crowded cytoplasmic environment, with about half of the volume estimated to be occupied by protein and other macromolecules [44]. Another consequence of the crowded cytoplasm is that the phage DNA is compacted, as a result of DNA condensation induced by osmotic stress [36] and/or nonspecific binding by nucleoid-associated proteins [37,38], and we approximate the compacted phage DNA as a blob of hydrodynamic radius  $R_H$  [see the Fig. 1(b) inset and Refs. [36,49] for experimental observations of single or multiple phage DNA molecules compacted into blobs of a few hundred nm in crowded *in vitro* conditions). The state of the DNA is reflected in its  $R_H$  as a function of the DNA length N (base pairs), given by  $R_H \propto N^{\gamma}$  [50]. In good solvents and without other effects, the DNA can be

modeled as a self-avoiding Gaussian chain, and  $\gamma = 3/5$ . On the other hand, if the DNA is in a collapsed state, the volume of a DNA blob is proportional to the number of base pairs, and  $\gamma = 1/3$ . Taking the persistence length  $\xi_p$  as the segment size for both cases, we have  $R_H = \xi_p (bN/\xi_p)^{\gamma}$ , with  $b \approx 0.34$  nm the size of a nucleotide in double-stranded DNA. In other words, we find

$$R_H = \xi_p^{1-\gamma} b^{\gamma} N^{\gamma}. \tag{4}$$

Typically, the persistence length is  $\xi_p \approx 50$  nm for DNA in cells [44] and  $N \approx 50$  kbp for phage  $\lambda$  DNA. If  $\gamma = 3/5$ , then  $R_H \approx 1650$  nm, which would exceed the width of an  $E.\ coli$  cell (roughly 1  $\mu$ m). For  $\gamma = 1/3$ ,  $R_H \approx 350$  nm is smaller than the cell size so, hereafter, we will assume that the phage DNA in the cell is a compacted blob and set  $\gamma = 1/3$ , consistent with previous experimental evidence that the injected phage DNA remains near the site of entry in the collapsed state [34,36,51].

As ejection progresses, DNA newly released into the cell is expected to collapse onto the blob. To estimate the amount of ejected DNA,  $N \equiv \sqrt{\langle N^2(t) \rangle}$  (in base pairs), we identify it with the MSD $\langle r^2 \rangle$  of the subdiffusive motion of the blob as a whole. Here, we define  $\langle r^2 \rangle$  to be the sum of all the squared displacements where movement of the blob is coupled to the release of DNA,

$$\langle r^2 \rangle \equiv b^2 \langle N^2(t) \rangle = b^2 N^2.$$
 (5)

With that assumption, we assert that the Brownian motion of the blob is coupled to the linear motion of the released base pairs. In other words, every displacement of the center of the blob away from the phage tail pulls out a similar length of DNA. Released parts of the DNA subsequently condense onto the blob, and the process continues with a growing blob until all the DNA has been released.

The subdiffusion of the DNA blob is given by

$$\langle r^2 \rangle = 6D[R_H(N(t))]t^{\alpha}, \tag{6}$$

where D is the long-time diffusion coefficient of the condensed DNA blob, depending on N through its hydrodynamic radius  $R_H$ . We assume that the Stokes-Einstein diffusion coefficient is the relevant quantity that sets the timescale for self-diffusion. That is,  $D[R_H(N(t))] \approx (k_B T/6\pi\eta)(1/R_H)$ , making D inversely proportional to  $R_H$  and the dynamic viscosity of the cytoplasm  $\eta$ . The viscosity of the cytoplasm  $\eta = f\eta_0$ , with  $f \approx 10$  (see above) and with the viscosity of water  $\eta_0$ . We define  $K_0 = (k_B T/6\pi\eta_0) \approx 2.15 \times 10^{-19} \text{ m}^3/\text{s}$  [44], and use  $R_H$  from Eq. (4), to find

$$D[R_H(N(t))] \approx f^{-1} K_0 \xi_p^{\gamma - 1} b^{-\gamma} N^{-\gamma}.$$
 (7)

Combining Eqs. (7) and (5) into Eq. (6), and defining  $\chi = (6f^{-1}K_0/b^{2+\gamma}\xi_p^{1-\gamma})$  and  $\omega = (\alpha/2 + \gamma)$ , we have

$$N(t) = \chi^{(1/2+\gamma)} t^{\omega}. \tag{8}$$

The speed is therefore  $\mathbf{v}=(dN/dt)=\omega\chi^{(1/2+\gamma)}t^{(\omega-1)},$  or  $\mathbf{v}=\omega\chi^{\{[1/(2+\gamma)]\cdot(1/\omega)\}}N^{[1-(1/\omega)]}.$  Taking  $\alpha=0.5$  and  $\gamma=1/3$  for the subdiffusing DNA blob, we have  $\omega=0.21,$  so  $N(t)=\chi^{0.43}t^{0.21},$  and the time derivative  $\mathbf{v}(t)=0.21\cdot\chi^{0.43}t^{-0.79}.$  Replacing t by t(N) in the expression for  $\mathbf{v}(t),$  we obtain  $\mathbf{v}=0.21\cdot\chi^{2.05}N^{-3.8}.$  If we use typical values  $b\approx0.34$  (nm/bp),  $\xi_p\approx50$  nm, and  $f\approx10$  for  $E.\ coli\ [44],$  then we expect  $\chi$  to be  $1.21\times10^8\ \mathrm{s}^{-1}.$ 

To compare with the measurement, Fig. 1(a) shows the in vivo ejection data in a log-log representation. The early, force-driven phase crosses over to a power-law behavior at about 25 kbp (10<sup>4.4</sup> bp)DNA ejected. Fitting the later stage gives  $\log v = (-3.99 \pm 1.67) \log N + (20.2 \pm 7.7)$ , or  $v = 10^{(20.2 \pm 7.7)} \cdot N^{(-3.99 \pm 1.67)}$ , where v and N are the ejection speed and the amount of DNA ejected and are in units bp/s and bp. Our model predicts  $v \propto N^{-3.8}$ , which is a very good prediction of the scaling. In addition, if we identify the constant in the v-N scaling,  $0.21 \cdot \chi^{2.05}$ , with the fitting parameter,  $10^{(20.2\pm7.7)}$ , we obtain  $\gamma = 2.7 \times 10^6$  $8.7 \times 10^{13}$  s<sup>-1</sup>. Our expected value [see the discussion below Eq. (8)] falls within this range, but we note that the fitting parameter has an uncertainty of  $10^{(\pm 7.7)}$ , and we do not attempt to draw quantitative conclusions about this number. With that caveat, we argue that subdiffusion of  $\lambda$ phage DNA underlies the later-stage phage ejection in vivo when the driving force is exhausted. We also note that this subdiffusion model leads to the amount of DNA in the cell, rather than the amount of DNA in the phage, being the natural variable that makes the cI60 and b221 speed data collapse [Fig. 1(a)].

# IV. DISCUSSION

The ejection kinetics of individual phages exhibit substantial noise [15]; we have not addressed these phenomena. A possible source of such noise is the cell-to-cell variability (e.g., in growth phase, size, content, and crowdedness), causing variation in parameters such as  $R_H$ ,  $\eta$ , and  $P_b$ . However, as shown in Ref. [33], (anomalous) diffusion of DNA with a well-defined size does not in itself indicate extensive cell-to-cell variation. Additional sources of noise may involve the existence of DNA knots in the packaged phage genome, local structuring, or phase transitions [52] of the phage DNA spool, affecting  $\mu_v$  in a topology-dependent manner [53–55]. DNA knots may also result in blockages during ejections that are compatible to the total ejection timescale [54–56]. This was speculated to be the origin of the frequently observed pausing during the in vitro ejection of phage T5 [52]. Events with pausing were also observed for  $\lambda$  in vivo ejection [15], although they were not the majority and were excluded from the data shown in Fig. 1(a). The frequency of paused ejection events may correlate with knotting probability and complexity, which depend on phage genome length and the degree of confinement [57]. If the ejection pauses indeed reflect the untying of DNA knots, we expect that, outside of the paused regions, these events would have the same dynamics as described here. Another irregular ejection behavior observed in Ref. [15] is that, in the short-genome phage b221, about 36% of ejection events "stall" and never resume during the 30-min experiment. These stalled events were also excluded from the data shown in Fig. 1(a), as they may reflect phage particles with capsid defects [58,59]. The currently available data are insufficient to address separately all these effects, and it would be of considerable interest to examine the variability of ejection dynamics in more detail in the future.

Finally, we discuss some features of the theory for future investigations. It was found that the cytoplasmic subdiffusive behavior strongly depends on the homeostasis of the cells [32,33,48]. These studies suggest that the meansquared displacement of macromolecules in bacterial cytoplasm is significantly reduced but does not vanish in metabolically inactive cells. As a consequence, we expect that phage ejection will be significantly slowed down in that situation. Also, implicit in our model is that water and ions must enter the semipermeable phage capsid (permeable for water and small ions, not for macromolecules) to compensate for DNA ejection. In the case of phage ejection into a solution containing high-molecular-weight osmolyte (e.g., polyethylene glycol), the osmolyte effectively pulls on the water in the capsid, putting it under tension that limits the extent of ejection of the DNA [3,25,26]. Analogously, when herpes viruses infect eukaryotic cells, their genomes enter the nuclei, while their capsids remain in the cytoplasm, and current evidence suggests that this genome translocation may be driven by the pressurized viral DNA in the capsid [16,60]. Moreover, macromolecules are suggested to exhibit subdiffusion in the eukaryotic nuclei as well [61,62]. Although additional biological mechanisms may be necessary to explain the nuclear entry of herpes viruses [63], it would be interesting to consider the theoretical elements presented here in this process and take into account the high-osmolarity cytoplasmic surrounding of the capsids.

Our finding of the importance of anomalous diffusion in living cells transcends the field of viral DNA translocation. Viral genome delivery is one of the many realizations of polymer translocation, which includes important biological processes such as bacterial conjugation, protein trafficking to various organelles, messenger RNA translocating through the nuclear pores, drug delivery using polymer carriers, etc. These systems are expected to exhibit translocation scaling behaviors manifested from the polymers'

subdiffusive characteristics, in a similar way as described here for viral genome translocation.

### **ACKNOWLEDGMENTS**

We are grateful to the late William Klug, David Van Valen, Mattias Rydenfelt, Arbel Tadmor, Ian Molineux, Maja Bialecka-Fornal, Heun Jin Lee, Timur Zhiyentayev, Long Cai, Stephanie Weber, Andrew Spakowitz, and Julie Theriot for helpful insights and discussions. This work was supported by La Fondation Pierre-Gilles de Gennes, the Rosen Center at Caltech, the James S. McDonnell Foundation, the National Institutes of Health DP1 OD000217 (Directors Pioneer Award), R01 GM085286 and 1R35 GM118043-01 (MIRA), F32 HL134288, the National Science Foundation Grants No. 1161803 and No. CHE1051507, and the Netherlands Organization for Scientific Research (NWO TOPGO grant).

- [1] A. Fokine and M. G. Rossmann, *Molecular Architecture of Tailed Double-Stranded DNA Phages*, Bacteriophage 4, e28281 (2014).
- [2] J. Kindt, S. Tzlil, A. Ben-Shaul, and W. M. Gelbart, DNA Packaging and Ejection Forces in Bacteriophage, Proc. Natl. Acad. Sci. U.S.A. 98, 13671 (2001).
- [3] S. Tzlil, J. T. Kindt, W. M. Gelbart, and A. Ben-Shaul, Forces and Pressures in DNA Packaging and Release from Viral Capsids, Biophys. J. 84, 1616 (2003).
- [4] P. K. Purohit, J. Kondev, and R. Phillips, *Mechanics of DNA Packaging in Viruses*, Proc. Natl. Acad. Sci. U.S.A. 100, 3173 (2003).
- [5] P. K. Purohit, M. M. Inamdar, P. D. Grayson, T. M. Squires, J. Kondev, and R. Phillips, Forces during Bacteriophage DNA Packaging and Ejection, Biophys. J. 88, 851 (2005).
- [6] X. Qiu, D. C. Rau, V. A. Parsegian, L. T. Fang, C. M. Knobler, and W. M. Gelbart, Salt-Dependent DNA-DNA Spacings in Intact Bacteriophage λ Reflect Relative Importance of DNA Self-Repulsion and Bending Energies, Phys. Rev. Lett. 106, 028102 (2011).
- [7] Z. T. Berndsen, N. Keller, S. Grimes, P. J. Jardine, and D. E. Smith, *Nonequilibrium Dynamics and Ultraslow Relaxation of Confined DNA during Viral Packaging*, Proc. Natl. Acad. Sci. U.S.A. 111, 8345 (2014).
- [8] I. L. Ivanovska, R. Miranda, J. L. Carrascosa, G. J. Wuite, and C. F. Schmidt, *Discrete Fracture Patterns of Virus Shells Reveal Mechanical Building Blocks*, Proc. Natl. Acad. Sci. U.S.A. 108, 12611 (2011).
- [9] W. H. Roos, I. Gertsman, E. R. May, C. L. Brooks, J. E. Johnson, and G. J. Wuite, *Mechanics of Bacteriophage Maturation*, Proc. Natl. Acad. Sci. U.S.A. 109, 2342 (2012).
- [10] D. E. Smith, Single-Molecule Studies of Viral DNA Packaging, Curr. Opin. Virol. 1, 134 (2011).
- [11] D. N. Fuller, D. M. Raymer, J. P. Rickgauer, R. M. Robertson, C. E. Catalano, D. L. Anderson, S. Grimes, and D. E. Smith, Measurements of Single DNA Molecule Packaging Dynamics in Bacteriophage λ Reveal High Forces, High Motor

- Processivity, and Capsid Transformations, J. Mol. Biol. 373, 1113 (2007).
- [12] D. N. Fuller, D. M. Raymer, V. I. Kottadiel, V. B. Rao, and D. E. Smith, Single Phage T4 DNA Packaging Motors Exhibit Large Force Generation, High Velocity, and Dynamic Variability, Proc. Natl. Acad. Sci. U.S.A. 104, 16868 (2007).
- [13] J. P. Rickgauer, D. N. Fuller, S. Grimes, P. J. Jardine, D. L. Anderson, and D. E. Smith, *Portal Motor Velocity and Internal Force Resisting Viral DNA Packaging in Bacteriophage ф*29, Biophys. J. **94**, 159 (2008).
- [14] N. Keller, S. Grimes, P. J. Jardine, and D. E. Smith, *Repulsive DNA-DNA Interactions Accelerate Viral DNA Packaging in Phage*  $\phi$ 29, Phys. Rev. Lett. **112**, 248101 (2014).
- [15] D. Van Valen, D. Wu, Y.-J. Chen, H. Tuson, P. Wiggins, and R. Phillips, *A Single-Molecule Hershey-Chase Experiment*, Curr. Biol. **22**, 1339 (2012).
- [16] D. W. Bauer, J. B. Huffman, F. L. Homa, and A. Evilevitch, Herpes Virus Genome, the Pressure Is On, J. Am. Chem. Soc. 135, 11216 (2013).
- [17] K. Hanhijärvi, G. Ziedaite, M. Pietilä, E. Hæggström, and D. Bamford, DNA Ejection from an Archaeal Virus—A Single-Molecule Approach, Biophys. J. 104, 2264 (2013).
- [18] D. Rau, B. Lee, and V. Parsegian, Measurement of the Repulsive Force between Polyelectrolyte Molecules in Ionic Solution: Hydration Forces between Parallel DNA Double Helices, Proc. Natl. Acad. Sci. U.S.A. 81, 2621 (1984).
- [19] M. M. Inamdar, W. M. Gelbart, and R. Phillips, *Dynamics of DNA Ejection from Bacteriophage*, Biophys. J. **91**, 411 (2006).
- [20] L. R. Garcia and I. J. Molineux, Rate of Translocation of Bacteriophage T7 DNA across the Membranes of Escherichia Coli, J. Bacteriol. 177, 4066 (1995).
- [21] P. Kemp, M. Gupta, and I. J. Molineux, *Bacteriophage T7 DNA Ejection into Cells Is Initiated by an Enzyme-Like Mechanism*, Mol. Microbiol. **53**, 1251 (2004).
- [22] V. González-Huici, M. Salas, and J. M. Hermoso, The Push-Pull Mechanism of Bacteriophage φ29 DNA Injection, Mol. Microbiol. 52, 529 (2004).
- [23] W. Roos, I. Ivanovska, A. Evilevitch, and G. Wuite, *Viral Capsids: Mechanical Characteristics, Genome Packaging and Delivery Mechanisms*, Cell Mol. Life Sci. **64**, 1484 (2007).
- [24] A. Bertin, M. de Frutos, and L. Letellier, *Bacteriophage-Host Interactions Leading to Genome Internalization*, Curr. Opin. Microbiol. **14**, 492 (2011).
- [25] A. Evilevitch, L. Lavelle, C. M. Knobler, E. Raspaud, and W. M. Gelbart, *Osmotic Pressure Inhibition of DNA Ejection from Phage*, Proc. Natl. Acad. Sci. U.S.A. **100**, 9292 (2003).
- [26] P. Grayson, A. Evilevitch, M. M. Inamdar, P. K. Purohit, W. M. Gelbart, C. M. Knobler, and R. Phillips, *The Effect of Genome Length on Ejection Forces in Bacteriophage λ*, Virology 348, 430 (2006).
- [27] P. Grayson, L. Han, T. Winther, and R. Phillips, *Real-Time Observations of Single Bacteriophage λ DNA Ejections In Vitro*, Proc. Natl. Acad. Sci. U.S.A. **104**, 14652 (2007).
- [28] D. Wu, D. Van Valen, Q. Hu, and R. Phillips, *Ion-Dependent Dynamics of DNA Ejections for Bacteriophage λ*, Biophys. J. **99**, 1101 (2010).

- [29] J. Stock, B. Rauch, and S. Roseman, *Periplasmic Space in Salmonella Typhimurium and Escherichia Coli*, J. Biol. Chem. **252**, 7850 (1977).
- [30] Y. Deng, M. Sun, and J. W. Shaevitz, *Direct Measurement of Cell Wall Stress Stiffening and Turgor Pressure in Live Bacterial Cells*, Phys. Rev. Lett. **107**, 158101 (2011).
- [31] C. São-José, M. de Frutos, E. Raspaud, M. A. Santos, and P. Tavares, Pressure Built by DNA Packing inside Virions: Enough to Drive DNA Ejection In Vitro, Largely Insufficient for Delivery into the Bacterial Cytoplasm, J. Mol. Biol. 374, 346 (2007).
- [32] S. C. Weber, A. J. Spakowitz, and J. A. Theriot, *Bacterial Chromosomal Loci Move Subdiffusively through a Viscoelastic Cytoplasm*, Phys. Rev. Lett. **104**, 238102 (2010).
- [33] B. R. Parry, I. V. Surovtsev, M. T. Cabeen, C. S. O'Hern, E. R. Dufresne, and C. Jacobs-Wagner, *The Bacterial Cytoplasm Has Glass-Like Properties and Is Fluidized by Metabolic Activity*, Cell 156, 183 (2014).
- [34] A. Tal, R. Arbel-Goren, N. Costantino, D. L. Court, and J. Stavans, *Location of the Unique Integration Site on an Escherichia Coli Chromosome by Bacteriophage λ DNA In Vivo*, Proc. Natl. Acad. Sci. U.S.A. **111**, 7308 (2014).
- [35] D. Löf, K. Schillén, B. Jönsson, and A. Evilevitch, *Forces Controlling the Rate of DNA Ejection from Phage \lambda*, J. Mol. Biol. **368**, 55 (2007).
- [36] M. Jeembaeva, M. Castelnovo, F. Larsson, and A. Evilevitch, *Osmotic Pressure: Resisting or Promoting DNA Ejection from Phage?*, J. Mol. Biol. **381**, 310 (2008).
- [37] J. Stavans and A. Oppenheim, DNA-Protein Interactions and Bacterial Chromosome Architecture, Phys. Biol. 3, R1 (2006).
- [38] R. de Vries, *DNA Condensation in Bacteria: Interplay between Macromolecular Crowding and Nucleoid Proteins*, Biochimie **92**, 1715 (2010).
- [39] J.-Z. Wang, L. Li, and H.-J. Gao, Compressed Wormlike Chain Moving out of Confined Space: A Model of DNA Ejection from Bacteriophage, Acta Mech. Sin. (Engl. Ed.) 28, 1219 (2012).
- [40] C. Stanley and D. C. Rau, Evidence for Water Structuring Forces between Surfaces, Curr. Opin. Colloid Interface Sci. 16, 551 (2011).
- [41] J. Faraudo and F. Bresme, *Origin of the Short-Range, Strong Repulsive Force between Ionic Surfactant Layers*, Phys. Rev. Lett. **94**, 077802 (2005).
- [42] J. Valle-Delgado, J. Molina-Bolivar, F. Galisteo-Gonzalez, M. Galvez-Ruiz, A. Feiler, and M. W. Rutland, *Hydration Forces between Silica Surfaces: Experimental Data and Predictions from Different Theories*, J. Chem. Phys. 123, 034708 (2005).
- [43] V. Parsegian and T. Zemb, *Hydration Forces: Observations, Explanations, Expectations, Questions*, Curr. Opin. Colloid Interface Sci. **16**, 618 (2011).
- [44] R. Milo and R. Phillips, *Cell Biology by the Numbers* (Garland Science, New York, 2015).
- [45] M9 buffer: 22-mM  $\rm KH_2PO_4$ , 47.7-mM  $\rm Na_2HPO_4$ , 2.5-mM  $\rm NaCl$ , 18.7-mM  $\rm NH_4Cl$ , 2-mM  $\rm MgSO_4$ , 0.1-mM  $\rm CaCl_2$ , and  $\rm 4(\it g/L)$  glucose or glycerol.
- [46] I. Golding and E. C. Cox, *Physical Nature of Bacterial Cytoplasm*, Phys. Rev. Lett. **96**, 098102 (2006).

- [47] J.-H. Jeon, V. Tejedor, S. Burov, E. Barkai, C. Selhuber-Unkel, K. Berg-Sørensen, L. Oddershede, and R. Metzler, In Vivo Anomalous Diffusion and Weak Ergodicity Breaking of Lipid Granules, Phys. Rev. Lett. 106, 048103 (2011).
- [48] S. C. Weber, A. J. Spakowitz, and J. A. Theriot, Nonthermal ATP-Dependent Fluctuations Contribute to the In Vivo Motion of Chromosomal Loci, Proc. Natl. Acad. Sci. U.S.A. 109, 7338 (2012).
- [49] V. Vasilevskaya, A. Khokhlov, Y. Matsuzawa, and K. Yoshikawa, Collapse of Single DNA Molecule in Poly (Ethylene Glycol) Solutions, J. Chem. Phys. 102, 6595 (1995).
- [50] M. Rubenstein and R. H. Colby, *Polymer Physics* (Oxford University Press, Oxford, 2003).
- [51] C. F. Earhart, The Association of Host and Phage DNA with the Membrane of Escherichia Coli, Virology 42, 429 (1970).
- [52] N. Chiaruttini, M. De Frutos, E. Augarde, P. Boulanger, L. Letellier, and V. Viasnoff, Is the In Vitro Ejection of Bacteriophage DNA Quasistatic? A Bulk to Single Virus Study, Biophys. J. 99, 447 (2010).
- [53] J. Arsuaga, M. Vázquez, S. Trigueros, and J. Roca, *Knotting Probability of DNA Molecules Confined in Restricted Volumes: DNA Knotting in Phage Capsids*, Proc. Natl. Acad. Sci. U.S.A. **99**, 5373 (2002).
- [54] R. Matthews, A. Louis, and J. Yeomans, *Knot-Controlled Ejection of a Polymer from a Virus Capsid*, Phys. Rev. Lett. **102**, 088101 (2009).
- [55] D. Marenduzzo, C. Micheletti, E. Orlandini, and D. W. Sumners, *Topological Friction Strongly Affects Viral DNA Ejection*, Proc. Natl. Acad. Sci. U.S.A. 110, 20081 (2013).
- [56] A. Rosa, M. Di Ventra, and C. Micheletti, Topological Jamming of Spontaneously Knotted Polyelectrolyte Chains Driven through a Nanopore, Phys. Rev. Lett. 109, 118301 (2012).
- [57] C. Micheletti, D. Marenduzzo, E. Orlandini, and D. Summers, *Knotting of Random Ring Polymers in Confined Spaces*, J. Chem. Phys. **124**, 064903 (2006).
- [58] I. Ivanovska, G. Wuite, B. Jönsson, and A. Evilevitch, Internal DNA Pressure Modifies Stability of WT Phage, Proc. Natl. Acad. Sci. U.S.A. 104, 9603 (2007).
- [59] S. Köster, A. Evilevitch, M. Jeembaeva, and D. A. Weitz, *Influence of Internal Capsid Pressure on Viral Infection by Phage λ*, Biophys. J. **97**, 1525 (2009).
- [60] I. Liashkovich, W. Hafezi, J. M. Kühn, H. Oberleithner, and V. Shahin, *Nuclear Delivery Mechanism of Herpes Simplex Virus Type 1 Genome*, J. Mol. Recognit. **24**, 414 (2011).
- [61] D. S. Banks and C. Fradin, Anomalous Diffusion of Proteins Due to Molecular Crowding, Biophys. J. 89, 2960 (2005).
- [62] I. Bronstein, Y. Israel, E. Kepten, S. Mai, Y. Shav-Tal, E. Barkai, and Y. Garini, *Transient Anomalous Diffusion of Telomeres in the Nucleus of Mammalian Cells*, Phys. Rev. Lett. 103, 018102 (2009).
- [63] N. Fay and N. Panté, Nuclear Entry of DNA Viruses, Front. Microbiol. 6, 467 (2014).

*Correction:* The fourth byline footnote contained a production error and has been fixed. Missing information in the Acknowledgments section has been inserted.